Fig. 2. Device cross section.

The fabrication process starts with active/passive definition using a wet etch, then gratings are patterned using electron beam lithography and etched. The waveguide p-cladding is regrown, then the surface ridge is defined by a dry etch with a cleanup wet etch. SiN is then deposited, followed by a SiO_2 patterning, leaving a 2.4 μm thick oxide layer for the detector contact pads. The vias through the oxide and nitride are etched, and p-metal is deposited, followed by isolation implantation, wafer thinning and back-side n-metal deposition. An AR coating was not applied to this device. The devices are then cleaved apart, mounted to a carrier and wire bonded; the PDs are wire bonded to 50Ω coplanar waveguide transmission lines.

3. Results

We first summarize the results of the receiver PIC component characterization. We then discuss the receiver performance with 20 Gb/s NRZ-QPSK signals.

3.1. SG-DBR local oscillator

The SG-DBR is evaluated in terms of wavelength tuning range, side-mode suppression ratio (SMSR), and linewidth. The SG-DBR wavelength tuning map is shown in Fig. 3(a), and was obtained by sweeping both front and back mirrors from 0 to 20 mA and measuring the peak wavelength in an OSA. As shown, the SG-DBR can be quasi-continuously tuned over 30 nm, from 1544 nm to 1577 nm. In single-mode operation, SMSR of up to 48 dB was measured and was observed to be typically greater than 40 dB. SG-DBR full width at half maximum (FWHM) linewidths of 105-156 MHz was measured using the heterodyne measurement at 3 dB down with a 100 kHz laser. Using spectral width data measured at 30 dB down, the free-running FWHM linewidth is estimated to be 17-25 MHz. The SG-DBR linewidth is dominated by low-frequency jitter [9] and this direct measurement of the SG-DBR linewidth also measures noise from the current sources used to bias the laser. The linewidth can be further reduced with the use of capacitors to stabilize the SG-DBR biases.

3.2. Photodetectors

The photodetector frequency response was measured with a 20 GHz LCA (Lightwave Component Analyzer) output, amplified to 10 dBm, and then coupled into the receiver PIC with a lensed fiber. Inputs SOA1 and SOA2 were biased to 40mA and 100mA, respectively. The PD CPW line was contacted with a GSG RF probe and reversed biased through a bias tee to −3V. The RF signal from the PD was connected to the LCA through the bias tee. The frequency response for all 4 detectors is shown in Fig. 3(b) showing detector 3-dB bandwidths of 10 GHz, sufficient for 10 Gbaud signals. With all PIC components biased, the dark current on each photodetector is 19 μA at a reverse bias of 3V.
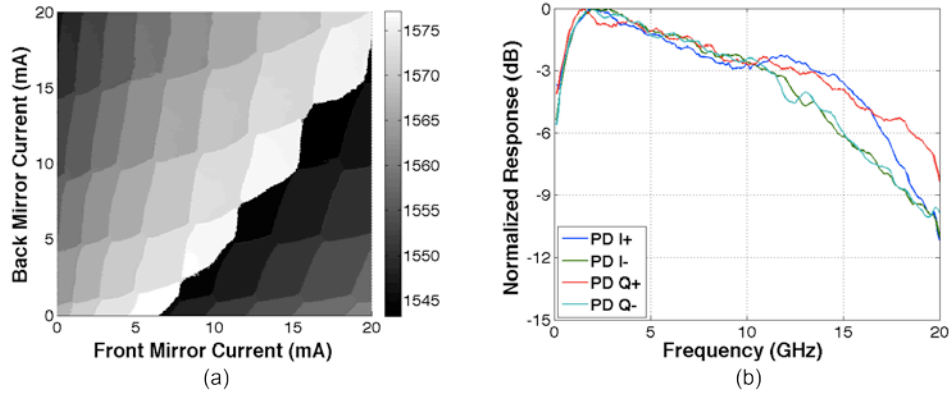
Fig. 3. (a) SG-DBR wavelength (nm) vs. bias currents of front and back mirrors showing quasi-continuous tuning range of over 30 nm. Photodetector normalized frequency response (b) of all four photodetectors.

3.3. 90° optical hybrid

The optical hybrid is composed of four tunable MMIs and four phase shifters. The phase of the hybrid was characterized using the method described in [10]. In our case, we mixed the SG-DBR output with CW light tuned close to the SG-DBR wavelength in the optical hybrid, and used the on-chip PDs to observe the beat signals in a real-time sampling oscilloscope. With this method we were able to tune the hybrid to 90° by biasing one phase shifter to 8.65 mA. Biasing the phase shifter to 4.72 mA and 16.38 mA tunes the hybrid to 0° and 180°, respectively.

A single tunable MMI and its tuning contact pads are shown in Fig. 4(a); P1 tunes the lower section of the MMI and P2 tunes the upper section. Figure 4(b) shows the power imbalance of the two outputs of a tunable MMI test structure without tuning is close to 0 dB, and with approximately 2 mA on P1, the two outputs can be perfectly balanced. Sweeping each tuning pad 20 mA, we see that we can unbalance the outputs of the MMI by over 5 dB. The power imbalance of a 90° optical hybrid, with and without tuning, was measured for a wavelength range of 1510 nm to 1630 nm, and is shown in Fig. 4(c). Without tuning, the power balance is below 2 dB for the entire wavelength range. By tuning the MMIs in the 90° optical hybrid, we are able to balance the outputs at a given wavelength.
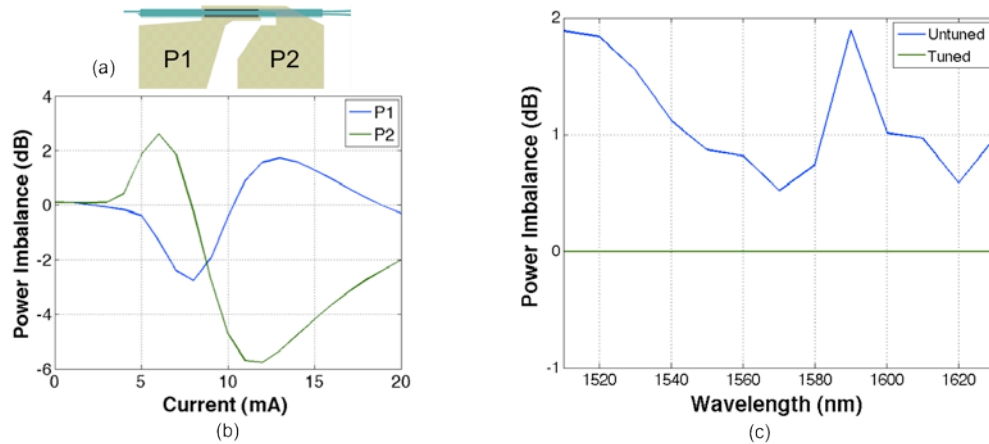

Fig. 4. Single tunable MMI bias pad configuration (a) and power imbalance tuning (b). 90° optical hybrid untuned and tuned power imbalance (c). With tuning the power imbalance is eliminated for the tested wavelength range of 1510 nm to 1630 nm.

3.4. Net responsivity

In order to determine the wavelength dependence of the receiver as a whole, we look at average net responsivity to a single photodetector as shown in Fig. 5. In this case, the net responsivity includes input coupling loss, gain from the preamplifier SOAs, loss in the 90° optical hybrid, and photodetector imperfections. Note that the 90° optical hybrid loss also includes the inherent 6-dB loss of the hybrid, splitting from one input to four outputs. SOA1 is biased at 40 mA and SOA2 is biased at 100 mA, and the photodetectors are reversed biased at −3V. The net responsivity is at a maximum of 0.17 A/W at 1545 nm and has a 3-dB bandwidth of 50 nm, from 1520 nm to 1570 nm. The roughness of the curve is attributed to slight changes in input fiber coupling during the measurement.
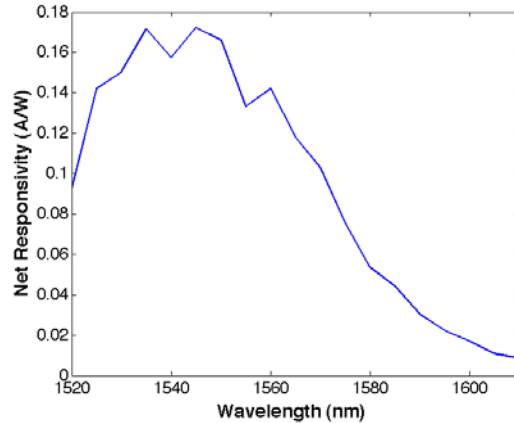

Fig. 5. Net Responsivity from fiber to a single photodetector, including input coupling loss, preamplifier gain, 90° optical hybrid loss, and photodetector imperfections. The 3-dB bandwidth is 50 nm.

3.5. Receiver performance

The experimental setup for 20 Gb/s NRZ-QPSK is shown in Fig. 6. CW output from a tunable laser was modulated by a QPSK LiNbO$_3$ modulator, driven by 10 Gb/s PRBS data on one arm and a delayed inverted data sequence on the other. The OSNR is set with a variable optical attenuator (VOA) and an EDFA. The signal was then pre-amplified by another EDFA, filtered, and input into the PIC with a lensed fiber. The pre-amplifier EDFA was set to a constant output power of approximately 8 dBm. The experimental setup is limited to the C band due to use of C band EDFAs and tunable filters. Other than the bias for the 90° phase shift, no other tuning was done to the optical hybrid. The single-ended I + (S + LO) and Q + (S + jLO) are input into the Agilent Optical Modulation Analyzer (OMA) N4391A. The OMA performs the necessary signal processing and features a real counting BER.
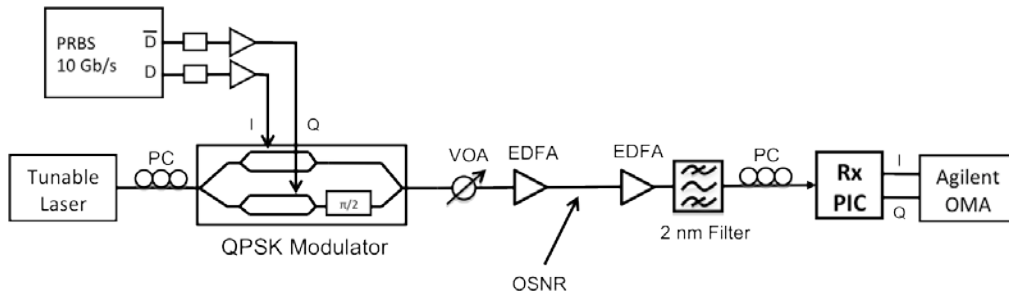

Fig. 6. Experimental setup.

As shown in Fig. 7(a), BER vs. OSNR measurements were performed with PRBS 2^7-1 data with input signal wavelengths of 1546.35, 1549.62, 1553.14, and 1556.75 nm and also with PRBS 2^{15}-1 data at 1549.89 nm. Current adjustment of only the back mirror is needed to tune the SG-DBR to these wavelengths. Similar performance is shown for all 5 cases. The required OSNR for BER of 10^{-3} is 10 dB, which is approximately 4 dB from the theoretical limit. An error floor is observed at 8×10^{-6} and indicates that without a feedback loop for the SG-DBR wavelength, long-term stability is an issue. A sample QPSK constellation displayed by the OMA is shown in Fig. 7(b) for an OSNR of 20 dB.
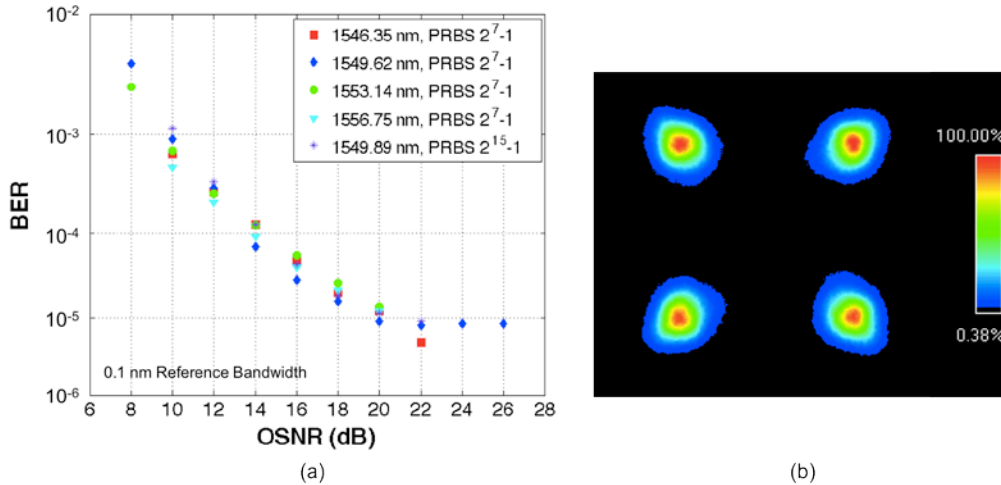

(a)   (b)

Fig. 7. BER vs. OSNR (a) and sample constellation at 20 dB OSNR (b). The required OSNR for BER of 10^{-3} is 10 dB.

4. Conclusions

We demonstrated an integrated coherent receiver with a monolithically integrated widely-tunable SG-DBR local oscillator, input SOAs, a 90° optical hybrid, and 10 GHz 3dB bandwidth photodetectors. The SG-DBR has a tuning range of over 30 nm with SMSR of over 40 dB and linewidths of 105-156 MHz. The net responsivity of the receiver has a 3-dB bandwidth of 50 nm. The receiver was tested with 20 Gb/s NRZ-QPSK for four different wavelengths, demonstrating a required OSNR of 10 dB for BER of 10^{-3}. For further improvement on receiver performance, on-carrier capacitors for the SG-DBR and photodetectors, dual-differential TIAs for balanced detection, and a feed-back loop for wavelength control can be implemented.

Acknowledgments